

## Model of H<sub>2</sub>S Catalytic Oxidation in an IAC–PBR

Federico Pugliese<sup>a,\*</sup>, Laura Merello<sup>a</sup>, Ezio Saturno<sup>b</sup>, Alberto Servida<sup>c</sup>, Paola Costamagna<sup>c</sup>

<sup>a</sup> Department of Civil, Chemical and Environmental Engineering, University of Genova, Via Opera Pia 15, I-16145 Genova (Italy)

<sup>b</sup> EXXRO S.r.l., Lungobisagno Istria 14, I-16141 Genova (Italy)

<sup>c</sup> Department of Chemistry and Industrial Chemistry, University of Genova, Via Dodecaneso 31, I-16146 Genova (Italy)

[federico.pugliese@edu.unige.it](mailto:federico.pugliese@edu.unige.it)

We focus our attention on hydrogen sulphide (H<sub>2</sub>S), which originates from various sources and is one of the major air pollutants. Concentrations above 140 mg m<sup>-3</sup> are immediately harmful for human health. Below that threshold, H<sub>2</sub>S is an odorous compound, which can be detected by human beings in concentration higher than 5 µg m<sup>-3</sup>. Its removal is conventionally performed through scrubbing with amine or NaOH aqueous solutions. Adsorption on activated carbons is an alternative technique, particularly suitable for application in the low H<sub>2</sub>S concentration range, being a typical example of odour removal technique. In this work, we propose a model of packed bed reactor (PBR) embedding impregnated activated carbons (IACs), where the H<sub>2</sub>S adsorption involves a catalytic partial oxidation step causing the deposition of elemental sulphur on the catalyst, with consequent gradual deactivation. The model equations are integrated numerically through the software COMSOL Multiphysics 5.3a. Simulation results are validated through comparison with literature experimental data. Furthermore, application to an industrial case study is presented and discussed.

### 1. Introduction

Problems associated with odour removal from air have become controversial issues, especially in urban areas (Turk et al., 1989). Sewage sludge treatment, sanitation facilities, and landfills are responsible for the majority of odorous emissions (Naddeo et al., 2016). In this framework, the removal of H<sub>2</sub>S is necessary also for concentrations below the limits of harmfulness to human health. The technologies available to remove H<sub>2</sub>S from gas streams can be classified into two general categories: (i) physical-chemical processes (chemical/physical absorption and adsorption); and (ii) biological processes (Abdullah et al., 2017). The choice between the previously described methods is mainly a function of the H<sub>2</sub>S concentration. A typical process scheme consists in a preliminary scrubber followed by an activated carbon (AC) packed bed reactor (PBR), where the AC bed adsorbs the H<sub>2</sub>S (Turk et al., 1992). Because of their relatively lower affinity to H<sub>2</sub>S, the application of unimpregnated AC is limited (Abatzoglu and Boivin, 2009). Indeed, for a cost-effective removal, the adsorption capacities and the removal rates must be substantially boosted through impregnation of the AC with suitable chemicals. In this way, the removal mechanism changes from adsorption to chemisorption. The chemical reaction taking place over the impregnated activated carbon (IAC) is the oxidation of H<sub>2</sub>S to elemental sulphur (Bandosz and Le, 1998):



Many chemicals can be used as impregnants; among them, KI displays the most interesting features in terms of increased reaction velocity and also inhibition of sulphuric acid formation by unwanted side-reactions (Henning and Schiifer, 1993). As reported by several authors (Bandosz and Le, 1998; Bouzaza et al., 2004; Wang et al., 2006), the chemical reaction is the rate determining step (RDS) of the overall process.

For the design of IAC-PBRs adsorption beds, two different approaches can be used: direct experimentation or mathematical modelling. The former mainly aims at providing the breakthrough curve (i.e. the effluent concentration vs. time profile). The latter involves the solution of the conservation, transport, and

thermodynamic equilibrium equations, consisting in a set of coupled partial differential and algebraic equations (PDAEs), which must be solved using numerical techniques. The final goal, again, is to determine the breakthrough curve.

The aim of the present work is to develop an IAC-PBR modelling tool, applicable for inlet H<sub>2</sub>S concentrations <5 mg m<sup>-3</sup> (odour range), which can predict the breakthrough curve by modelling the dynamics of (i) the H<sub>2</sub>S adsorption within the IAC-PBR, and (ii) the deactivation of the IAC bed. In the present work, ACs impregnated with KI are considered.

## 2. IAC-PBR model

### 2.1 Model equations

The model is based on the following assumptions: (i) tubular IAC-PBR reactor; (ii) time-dependent 1-D model along the reactor axial co-ordinate  $z$ ; (iii) ideal plug-flow behaviour; and (iv) isothermal conditions. The model includes the mass balance for the gas and the solid phase, coupled to a rate law for Reaction 1. More in detail, Eq(1) below is the mass balance for H<sub>2</sub>S in the gas phase, while Eq(2) is the mass balance for S being deposited onto the solid phase:

$$\frac{\partial C}{\partial t} + u \frac{\partial C}{\partial z} - D \frac{\partial^2 C}{\partial z^2} = - \frac{1 - \varepsilon}{\varepsilon} \rho_{ctl} \eta R \quad (1)$$

$$\frac{\partial C_p}{\partial t} = \rho_{ctl} \eta R \quad (2)$$

where:  $C$  is the H<sub>2</sub>S concentration in the gas phase (g m<sup>-3</sup>),  $C_p$  is the S concentration in the solid phase (i.e. the IAC) (g m<sup>-3</sup>),  $t$  is the time (s),  $u$  is the gas velocity (m s<sup>-1</sup>),  $D$  is the diffusion coefficient (m<sup>2</sup> s<sup>-1</sup>),  $\varepsilon$  is the void fraction (–),  $\rho_{ctl}$  is the bulk density of the IAC (g<sub>ctl</sub> m<sup>-3</sup>),  $R$  is the reaction rate (g g<sub>ctl</sub><sup>-1</sup> s<sup>-1</sup>), and  $\eta$  is the catalyst effectiveness factor (–). It is worthwhile mentioning that  $\eta$  is a function of the Thiele modulus (Bird et al., 2007), which is the ratio between the characteristic times of reaction and diffusion processes. For the simplified model we deal with, we assume that  $\eta$  is constant along the entire reactor. This is rigorously correct only for a first order reaction rate. In the present work, the mass transfer resistances in the boundary layer outside the catalyst particle, and within the internal pores inside the catalytic particle, are all neglected, and it is assumed  $\eta = 1$ .

Concerning the reaction rate  $R$ , it must be born in mind that the shape of the equilibrium isotherm determines the shape of the breakthrough curve. Therefore, accurate assumption of the isotherm and mass transfer phenomena are fundamental. A monomolecular Langmuir-Hinshelwood (L-H) model is used to represent the overall process of oxidation-adsorption (Gutiérrez Ortiz et al., 2014). In addition, the deposited sulphur strongly influences the reaction rate, which decreases with the increase of the sulphur deposition. Accordingly, a deactivation term is included in the L-H reaction rate model (Bouzaza et al., 2004):

$$R = k_{H_2S} \frac{K_{H_2S} C}{\rho_{ctl} + K_{H_2S} C} \left( 1 - \frac{C_p}{\rho_{ctl} C_p^\infty} \right)^2 \quad (3)$$

where:  $k_{H_2S}$  is the reaction rate constant (g g<sub>ctl</sub><sup>-1</sup> s<sup>-1</sup>),  $K_{H_2S}$  is the adsorption coefficient (g<sub>ctl</sub> g<sup>-1</sup>), and  $C_p^\infty$  is the maximum S adsorption capacity of the IAC (g<sub>S</sub> g<sub>ctl</sub><sup>-1</sup>). The values of the reaction rate and of the adsorption constants are calculated as a function of the relative humidity (RH), according to the data from Wang et al. (2006). Furthermore, the value of the diffusion coefficient is taken from Aguilera et al. (2016).

### 2.2 Model integration in COMSOL Multiphysics 5.3a

The dynamic model resulting from Eq(1) and Eq(2) is implemented in COMSOL Multiphysics (version 5.3a) using the Chemical Engineering Module and the interface of Transport of Diluted Species (COMSOL Inc., 2018). Suitable initial conditions and boundary conditions are:

$$t = 0 \quad C = 0, \quad C_p = 0 \quad (4)$$

$$t > 0, \quad z = 0 \quad C = C_0 \quad (5)$$

$$t > 0, \quad z = L \quad \frac{\partial C}{\partial z} = 0 \quad (6)$$

where  $C_0$  is the H<sub>2</sub>S concentration in the feeding gas (g m<sup>-3</sup>). COMSOL Multiphysics employs the finite element method (FEM) method to solve the partial differential equations (PDEs) numerically. The resolution of

the equations is performed using the time dependent solver PARDISO. The simulations presented here, with a number of mesh elements of about 11000, typically run in 40 s on an Intel Xeon CPU with 64 GB of RAM.

### 3. Results and discussion

#### 3.1 Model validation

The simulation model is applied to the reactor described by Wang et al. (2006). Table 1 reports the values of the geometrical and physical-chemical parameters used as input data, including the adsorption capacity of the KI impregnated AC (Dalian Purit Co., Wang et al., 2006).

Table 1: Input data for the simulated IAC-PBR considered for model validation (Wang et al., 2006)

Parameter	Value	Unit	Parameter	Value	Unit
Reactor diameter	12.5	mm	Temperature	50	°C
Reactor length	550	mm	Bulk density	470	kg m <sup>-3</sup>
Feed gas flow rate (air)	500	Nml min <sup>-1</sup>	Diffusion coefficient	5.4	cm <sup>2</sup> s <sup>-1</sup>
			S adsorption capacity	6.9	mg <sub>S</sub> g <sub>cti</sub> <sup>-1</sup>

An evaluation of Reynolds ( $Re$ ) and Péclet ( $Pe$ ) dimensionless groups is made according to Eq(7) and Eq(8):

$$Re = \frac{\rho \cdot U_s \cdot d_p}{\mu} \quad (7)$$

$$Pe = \frac{U_s \cdot L}{\mathcal{D}} \quad (8)$$

where:  $\rho$  is the gas density (kg m<sup>-3</sup>),  $U_s$  is the superficial velocity (ratio between gas flow rate and cross sectional area) (m s<sup>-1</sup>),  $d_p$  is the catalyst particle diameter (m),  $\mu$  is the gas viscosity (kg m<sup>-1</sup> s<sup>-1</sup>), and  $L$  is the reactor length (m). Literature empirical correlations are used to determine the gas viscosity (Pooling et al., 2000). Based on the value of  $Re$  obtained by Eq(7), the flow can be laminar ( $Re < 10$ ), transitional ( $10 < Re < 300$ ) or turbulent ( $Re > 300$ ) (Ziolkowska and Ziolkowska, 1988). In the case under consideration,  $Re$  is about  $5.8 \cdot 10^3$ , and  $Pe$  is 70. Therefore, it is possible to conclude that in the present case the fluid flow is completely turbulent. In addition, the value of  $Pe$  indicates that diffusive effects are smaller than convective effects, and thus . In conclusion, this flow pattern is in full agreement with the plug-flow reactor hypothesis because convection is the prevailing effect within the reactor.

We wish to remark that the FEM method, implemented by COMSOL Multiphysics, is not well suited to convection – diffusion problems with negligible diffusion, as in the present case. In fact, the solution obtained is not stable. To overcome this problem, a variety of specialized numerical methods is available, as described by Finlayson (1992). COMSOL Multiphysics (version 5.3a) adds an artificial diffusion term to eliminate the oscillations in the solution without obscuring the essential details.

Simulation results are reported in Figure 1 and Figure 2. Figure 1(a) displays the gas phase H<sub>2</sub>S concentration profile along the reactor length, and Figure 1(b) displays the corresponding amount of S in the IAC. The lines represent the simulation results from 0 to 1 h with a time step of 0.1 h (i.e. 6 min). For longer simulations, the concentration profiles become flat and collapse with each other. Considering the profile at 0.5 h (yellow curve), it divides the reactor bed in three zones: (i) in the first part (between 0 to around 0.25 m) the IAC is completely saturated. In this situation, the H<sub>2</sub>S rich gas moves through the first zone without changing composition because no reaction takes place in this part of bed; (ii) in the intermediate part (0.25–0.3 m) the IAC contains S without being completely saturated. Here, the adsorption reaction takes place, and as a consequence the gas phase H<sub>2</sub>S concentration drops to zero, and (iii) in the final part of the reactor (from 0.3 to 0.55 m), the IAC is still virgin, but no reaction occurs since the gas phase H<sub>2</sub>S concentration is zero.

The results at different simulation times show the moving front of S saturation in the IAC (6.9 mg<sub>S</sub> g<sub>cti</sub><sup>-1</sup>), travelling from the entrance towards the exit of the reactor. The moving front of H<sub>2</sub>S concentration in the gas phase shows rather smooth edges, due to the contribution of the gas phase axial diffusion. Conversely, the moving front of S in the IAC is more vertical, due to the absence of solid phase S diffusion.

When the bed is completely saturated, the H<sub>2</sub>S concentration at the outlet is equal to the inlet one. Once the IAC bed reaches this condition, it is necessary to replace and dispose it. Therefore, in order to plan the IAC substitution in advance, it is important to know the breakthrough time. Figure 2 shows two simulated breakthrough curves corresponding to two different gas phase H<sub>2</sub>S inlet concentrations; the dots are literature experimental data (Wang et al., 2006). Both Figure 2(a) and (b) demonstrate good agreement between simulations and literature experimental data.

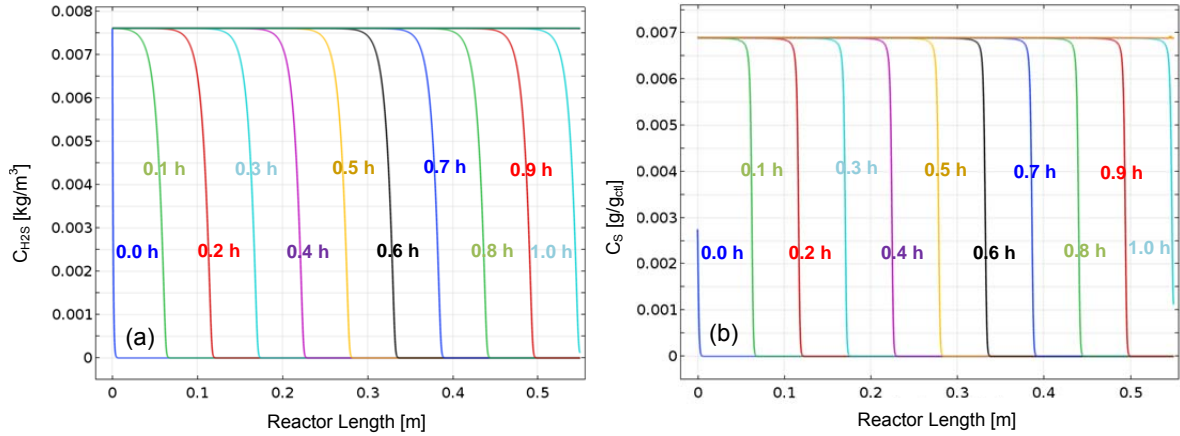


Figure 1: Simulation results for the IAC-PBR considered for model validation, input data in Table 1, inlet  $H_2S$  concentration  $C_0 = 7.6 \text{ g m}^{-3}$ ,  $RH = 20 \%$ . Simulation from 0 to 1 h with a time step 0.1 h: (a) gas phase  $H_2S$  concentration during time, and (b) S concentration profile in the IAC bed during time.

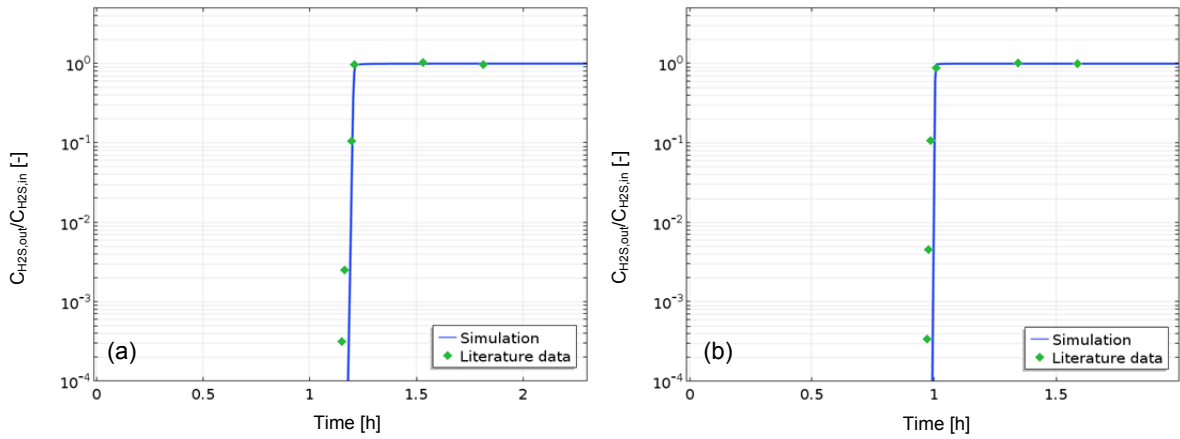


Figure 2: Simulation results for the IAC-PBR considered for model validation, input data in Table 1. Breakthrough curves for: (a) inlet  $H_2S$  concentration  $C_0 = 6.3 \text{ g m}^{-3}$ ,  $RH = 5 \%$ ; and (b) inlet  $H_2S$  concentration  $C_0 = 7.6 \text{ g m}^{-3}$ ,  $RH = 20 \%$ . Solid lines: COMSOL simulations; dots: literature experimental data (Wang et al. 2006).

### 3.2 Simplified calculation of breakthrough time

A simplified calculation, allowing to evaluate in a simple yet effective way the breakthrough time ( $t_B$ ), is reported in Eq(9). It is based on a macroscopic mass balance between the beginning of the reactor operation and the breakthrough time:

$$t_B = \frac{W_{ctl} \cdot C_p^\infty}{Q \cdot C_0 \cdot \frac{M_S}{M_{H_2S}}} \quad (9)$$

where:  $t_B$  is the breakthrough time (min),  $W_{ctl}$  is the catalyst weight (g),  $Q$  is the inlet volumetric gas flow rate ( $\text{m}^3 \text{ min}^{-1}$ ), and  $M_S$  and  $M_{H_2S}$  are the molar masses of S and  $H_2S$  respectively ( $\text{g mol}^{-1}$ ). Eq(9) is based on the assumption that the  $H_2S$  abatement is 100 % (i.e.  $H_2S$  outlet concentration of 0%). In order to check the validity of this equation, detailed COMSOL simulations are carried out varying the inlet  $H_2S$  concentration from 1 to  $7 \text{ g m}^{-3}$ , while maintaining the same operating conditions reported in Table 1. In the COMSOL simulations, the breakthrough time is considered to be achieved when the  $H_2S$  outlet concentration is 1 % of the inlet one. The results are reported in Figure 3. Figure 3(a) represents the different simulated breakthrough curves obtained by varying the inlet  $H_2S$  concentration from 1 to  $7 \text{ g m}^{-3}$ . Figure 3(b) displays a parity plot of the breakthrough time  $t_B$  calculated through Eq(9) and through the detailed COMSOL simulation, confirming that Eq(9) provides a reliable estimate of  $t_B$  in the window of operating conditions taken into consideration. For different values of the dimensionless numbers  $Re$ ,  $Pe$ , and Thiele modulus, the shape of the gas phase  $H_2S$  concentration profiles might be different, which could impact on the validity of Eq(9).

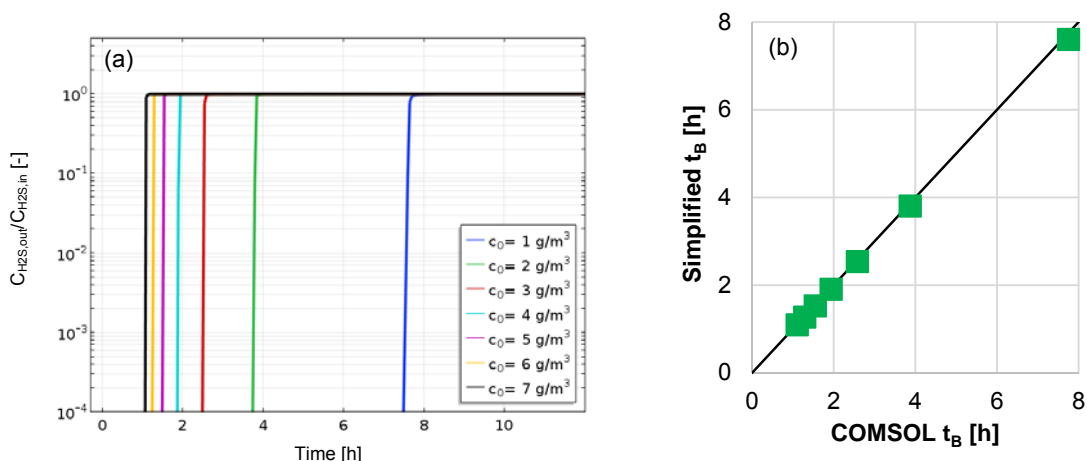


Figure 3: Simulation results for the IAC-PBR considered for model validation, input data in Table 1. (a) Breakthrough curves for  $H_2S$  inlet concentrations from 1 to 7  $g\ m^{-3}$ ,  $RH = 20\ %$ ; and (b) parity plot for the breakthrough time  $t_B$ .

### 3.3 Industrial case study: the EXXRO IAC-PBR

The model is applied to an IAC-PBR designed by EXXRO in order to treat the air in contact with leachate in the Grottaglie landfill (Taranto, Italy). The current configuration plant uses a caustic scrubber to reduce the gas phase  $H_2S$  significantly below 5  $mg\ m^{-3}$ . In this work, an additional treatment through an IAC-PBR is investigated in order to increase the global  $H_2S$  removal efficiency and to reduce the impact of the odour emissions. The operating parameters for this configuration are reported in Table 2, together with the chemical-physical properties of the KI IAC. The sulphur adsorption capacity is provided by the IAC supplier (COMELT S.p.A., 2018), and is significantly higher than that of the IAC considered for model validation. Indeed, this is a newly developed catalyst (COMELT S.p.A., 2018) with superior adsorption features.

Table 2: Input data for the simulated EXXRO IAC-PBR

Parameter	Value	Unit	Parameter	Value	Unit
Reactor diameter	800	mm	RH	40	%
Reactor length	1	m	Bulk density	1100	$kg\ m^{-3}$
Feed gas flow rate	500	$Nm^3\ h^{-1}$	Diffusion coefficient	5.4	$cm^2\ s^{-1}$
Temperature	20	$^{\circ}C$	S adsorption capacity	0.5	$g_s\ g_{cat}^{-1}$
Pressure	101.3	kPa	Inlet $H_2S$ concentration	5	$mg\ m^{-3}$

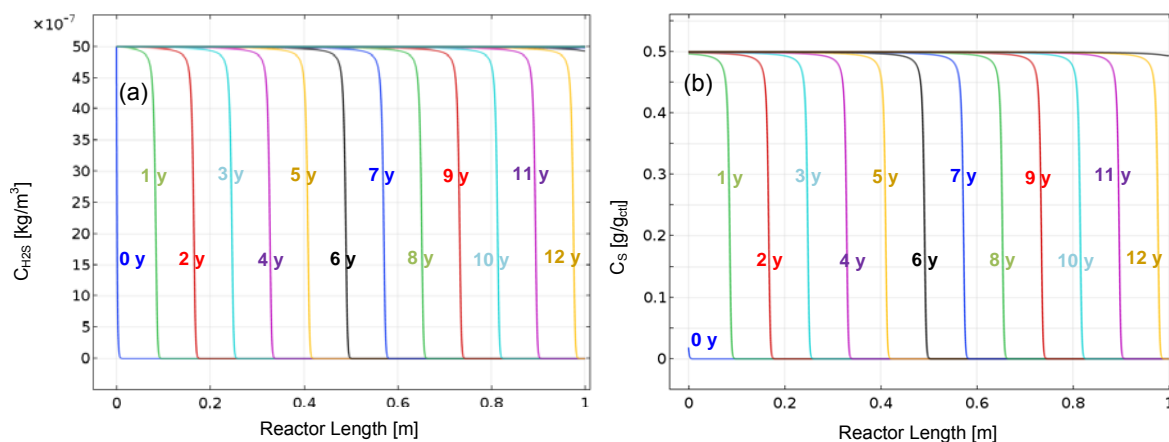


Figure 4: Simulation results for the EXXRO IAC-PBR, input data in Table 2. Simulation from 0 to 12 y with a time step of 1 y: (a) gas phase  $H_2S$  concentration during time, and (b) S concentration profile in the IAC bed during time.

Simulations are carried out considering the worst-case scenario of an inlet gas phase  $\text{H}_2\text{S}$  concentration of  $5 \text{ mg m}^{-3}$ . In this case, the scope of the IAC-PBR is just to eliminate the odorous emission. Simulation results are reported in Figure 4, which shows the profiles of gas phase  $\text{H}_2\text{S}$  concentration and of S concentration in the IAC bed during time. Being the  $\text{H}_2\text{S}$  inlet concentration very low ( $5 \text{ mg m}^{-3}$ ), the breakthrough time  $t_B$  is very long i.e. approximately 12 years. The value of  $t_B$  calculated using Eq(9) agrees with that provided by the detailed COMSOL simulation. It must be pointed out that the detailed COMSOL simulation can easily be extended to those (frequent) cases where the inlet  $\text{H}_2\text{S}$  concentration, as well as the overall gas flowrate, are variable during time.

#### 4. Conclusions and future work

The behavior of an IAC-PBR is studied through a model developed in COMSOL Multiphysics, version 5.3a. Firstly, the model is compared to previous literature results (Wang et al. 2006), obtaining good agreement. Then, the simulation of a small size industrial reactor is carried out to investigate the dynamics of (i) the  $\text{H}_2\text{S}$  adsorption within the IAC-PBR, and (ii) the deactivation of the IAC bed.

A simplified equation for the calculation of breakthrough time is proposed. Future work will focus on a detailed evaluation of the operating window where the simplified equation is applicable. To this end, the IAC-PBR behavior will be investigated, on the basis of the model, in a wide range of  $Re$ ,  $Pe$ , and Thiele modulus. In addition, the mass transport both in the boundary layer outside the catalyst particle, and within the pores of the catalytic particles, will be included in the model through the evaluation of the effectiveness factor  $\eta$ . Finally, the pressure drop caused by S adsorption will be considered as well.

#### References

- Abatzoglu N., Boivin S., 2009, A review of biogas purification, *Biofuels, Bioproducts & Biorefining*, 3, 42-71.
- Abdullah A.H., Mat R., Aziz A.S.A., Roslan F., 2017, Use of kaolin as adsorbent for removal of hydrogen sulfide from biogas, *Chemical Engineering Transactions*, 56, 763-768.
- Aguilera P.G., Gutiérrez Ortiz F.J., 2016, Prediction of fixed-bed breakthrough curves for  $\text{H}_2\text{S}$  adsorption from biogas: Importance of axial dispersion for design, *Chemical Engineering Journal*, 289, 93-98.
- Bandosz T., Le Q., 1998, Evaluation of surface properties of exhausted carbons used as  $\text{H}_2\text{S}$  adsorbents in sewage treatment plants, *Carbon*, 36, 39-44.
- Bird R.B., Stewart W.E., Lightfoot, E.N., 2007, *Transport Phenomena (Revised Second ed.)*, John Wiley & Sons, New York, NY-US.
- Bouzaza A., Laplanche A., Marsteau S., 2004, Adsorption–oxidation of hydrogen sulfide on activated carbon fibers: effect of the composition and the relative humidity of the gas phase. *Chemosphere*, 54, 481-488.
- COMELT S.p.A., 2018, <<https://www.comelt.it/prodotto/carbosorb-360-2ki-trattamento-aria-e-gas>> accessed 25.06.2018
- COMSOL Inc., 2018, *COMSOL Multiphysics Reference Manual*, version 5.3a, COMSOL Inc. <[www.comsol.com](http://www.comsol.com)> accessed 16.04.2018.
- Finlayson B.A., 1992, *Numerical methods for problems with moving fronts*, Ravenna Park Publishing Inc., Seattle, WA-US.
- Gutiérrez Ortiz F.J., Aguilera P., Ollero P., 2014, Modeling and simulation of the adsorption of biogas hydrogen sulfide on treated sewage–sludge, *Chemical Engineering Journal*, 253, 305–315.
- Henning K.D., Schiifer S., 1993, Impregnated activated carbon for environmental protection, *Gas Separation & Purification*, 7, 235-240
- Naddeo V., Zarra T., Oliva G., Chiavola A., Vivarelli A., 2016, Environmental odour impact assessment of landfill expansion scenarios: case study of Borgo Montello (Italy), *Chemical Engineering Transactions*, 54, 73-78.
- Poling B.E., Prausnitz J.M., O'Connell J.P., 2000, *The properties of gases and liquids*, McGraw-Hill, New York, NY-US.
- Turk A., Sakalis S., Lessuck J., Karamitsos H., Rago O., 1989, Ammonia injection enhances capacity of activated carbon for hydrogen sulfide and methyl mercaptan, *Environmental Science & Technology*, 33, 1242-1245.
- Turk A., Sakalis E., Rago O., Karamitsos H., 1992, Activated carbon systems for removal of light gases, *Annals of the New York Academy of Sciences*, 661,221-228.
- Wang L., Cao B., Wang S., Yuan Q., 2006,  $\text{H}_2\text{S}$  catalytic oxidation on impregnated activated carbon: Experiment and modelling, *Chemical Engineering Journal*, 118, 133-139.
- Ziolkowska I., Ziolkowska D., 1988, Fluid flow inside packed beds, *Chemical Engineering Process*, 23, 137-164.